Cutting Mechanics when Turning Powder Metallurgy Produced Nickel-Cobalt Base Alloy with a Cubic Boron Nitride Insert

Waldemar Daź[1*], Witold Habrat[2], Jarosław Tymczyszyn[2], Krzysztof Krupa[2]

[1] Pratt & Whitney Rzeszów S.A., ul. Hetmańska 120, 35-078 Rzeszów, Poland

[2] Politechnika Rzeszowska im. Ignacego Łukasiewicza, Al. Powstańców Warszawy 12, 35-959 Rzeszów, Poland

* Corresponding author's e-mail: daz_waldek@poczta.onet.pl

ABSTRACT

For the critical aero-engine parts it's important to understand influence of cutting tools, cutting parameters, tool wear etc. on near surface condition which highly affect fatigue strength and at the same part life-time. New material implemented for the latest designs of aero-engines parts generate challenges for machining processes to fulfil strict requirements of aviation standards. Finish machining is the most important stage of process influencing fatigue strength. Cubic Boron Nitride (cBN) tool are often used for final stage of machining. The objective of this study was analysis of cutting mechanics during finish turning of modern nickel-cobalt based alloy with cBN insert. Observations of cutting tool wear and cutting parameters influence on the components of cutting force, surface roughness and residual stress are presented in this paper.

Keywords: tool wear, cutting forces, surface roughness, nickel-cobalt based alloy, residual stress, cBN tool

INTRODUCTION

Since the first industrial use of nickel-based alloys for aircraft engine turbine blades in the 1940s, there has been continuous development in this area. Due to their good strength properties at elevated temperatures, corrosion resistance and creep resistance, nickel alloys have quickly become the primary structural materials used to manufacture hot zone components of aircraft engines [1–3]. However, the same characteristics that determine the excellent properties of nickel alloys at high temperatures negatively affect their machinability [4].

The composition of superalloys is primarily based on a combination of major alloying elements such as Iron Fe, Nickel Ni, Cobalt Co and Chromium Cr along with additives such as Tungsten W, Molybdenum Mo, Tantalum Ta; Niobium Nb, Titanium Ti and Aluminum Al [3]. Over the years, both the composition and fabrication methods of these materials have changed in order to improve the functional characteristics of the components made from them in terms of efficiency, performance and durability. Basically, three basic methods of obtaining superalloys can be distinguished. For all these methods, the initial phase of the manufacturing process is the same and consists of melting alloy elements and casting in the form of ingots. In a further process, the ingots are remelted and cast again or remelted and forged. The third method of producing nickel alloys is melting and atomization in the liquid state, forming a powder after solidification, which is then formed and subjected to sintering below the melting point and then forging [3]. The newest method based on powder metallurgy allows to obtain a new generation of superalloys based on nickel and cobalt with very favorable characteristics in terms of corrosion resistance, creep at high temperatures and strength, which has been presented in patent descriptions in relation to representatives of the previous generation of this type of alloys such as RENE 104 or IN100 [5,6].

Superalloys, because of their good mechanical and chemical properties at elevated temperatures,

are most commonly used in the aerospace, chemical, energy, and marine industries. Excellent structural properties such as strength, high temperature resistance, creep resistance, low thermal conductivity are challenging from the manufacturing point of view, because they cause high temperature in the cutting zone, the occurrence of large forces and stresses during cutting and strengthening of the surface layer. The phenomena accompanying the machining of superalloys cause rapid tool wear and the occurrence of many defects on the machined surface, negatively affecting the usability and operation of the manufactured components [3,7,8]. In general, superalloys belong to hard-to-machine materials due to the content of elements such as Ni, Co, Cr and Ti, and their machinability is at the level of a few to several % depending on the type of alloy [9].

The new method of manufacturing superalloys based on powder metallurgy and the composition of the alloy itself also have a significant impact on changing the machinability of these materials, and thus require the recognition of the mechanics of the cutting process to be able to effectively implement and control the machining process in terms of dimensions as well as quality and manufacturing costs. Despite these difficulties, machining remains the most common method of manufacturing products from HRSA materials, which significantly affects manufacturing costs and meeting the high quality requirements of manufactured components, especially in the aerospace industry [10]. The most important part of the process is the finish machining, which determines the properties of the near-surface consistency, which significantly affect the fatigue strength, part reliability and operating costs [11].

Aerospace standards specify near-surface parameters to be assessed and their limit values to ensure appropriate reliability and durability of aircraft engine components. Near-surface parameters are verified, among others, as deformation of the structure, including the form and depth or occurrence of the so-called "white layer", surface defects such as pulls, material tears, stuck chips, sharp tips, indentations and mismatches on certain surfaces (no traces of tool changes or merging of tool passes) [12].

Design requirements and the desired high machining efficiency and quality make modern ceramic tools, carbide tools with multilayer coatings and with a regular cubic Boron Nitride (cBN) Cutting Edge (CE) suitable for machining parts made of nickel-based superalloys. From a tool wear point of view, a characteristic feature in machining superalloys is a relatively short tool life, strongly dependent on the cutting speed. The higher cutting speed increases the temperature in the cutting zone and decreases the tool life. The forms of tool wear that are observed during machining of superalloys are mainly, build-up edge, temperature diffusion, grooving and abrasive wear [9,13]. The geometry has a significant influence on the machining of superalloys [3,14].

The practical experience of the aerospace industry in machining aircraft engine hot zone components indicates that the recommended allowance for finishing is not less than .030 inch (0.762 mm) and the recommended parameters: depth of cut ap and feed rate f .005–.003 inch (0.127 – 0.076 mm). The cutting speed v_c, depending on the tool material and the required length of cut (no faults and no traces of joining cuts), can vary over a wide range of values recommended by tool manufacturers.

Cutting tools during finishing operations often operate in the region of parameters a_p and f close to the values of parameters of the CE geometry of the tool. This significantly affects the machining process and the occurrence of side flow effect, Brammertz phenomenon and minimum thickness of the cut layer [15,16]. These phenomena strongly depend on the shape of the corner of the tool, the CE profile, the cutting parameters and the properties of the workpiece material and the cutting tool [16,17].

Hood et al [18], present a study of machining RR1000 superalloy with coated carbide tools. The study showed that for different cutting speeds v_c with a sharp tool, the best results were obtained in terms of surface layer quality, no visible defects were found, and the depth of surface layer deformation did not exceed 6 μm. At the worn tool $VB_{Bmax} \approx 0.2$ mm, surface defects appeared in the form of scuffing, rupture of material continuity (plucking, tear) and the depth of near surface deformation reached 20 μm.

Yao et al [19], in their published research materials, present a study stating that the cutting force occurring during machining of superalloys strongly depends on the depth of cut, slightly less on the feed rate, and is only slightly affected by the cutting speed. There is a clear dependence of the F_c component on a_p and f. Similarly, the component F_p behaves in relation to the changes of a_p and f.

Polvorosa et al. [4], in a study of superalloy machining (Waspaloy and Inconel 718), found that the size of the wear marks on the contact surface varies for the materials studied and these differences cannot be related to the cutting forces because they are identical in both cases. VB_N notch wear is the dominant form and determines the tool life.

According to Grzesik et al. [20], the main wear mechanism in the cutting of Inconel 718 is abrasive wear that causes grooving at the depth of the cut. The second wear mechanism is caused by the build-up edge on the rake face. Continuous measurement of the cutting force components during increasing tool wear has shown that there is some relationship between these values. In the finishing of the superalloy In 718 it is reasonable from the practical point of view to set the tool wear limit at $VB_{Bmax} \approx 0.2$ mm.

Sun et al. [21], while investigating the machining of nickel alloy GH4169, found that the machining parameters affect the properties of the near surface, in particular the roughness of the surface, the machining stresses and the transformations of the surface layer structure. They showed that lower cutting speeds with carbide tools produce a more favorable distribution of compressive stresses. This contributes to a reduction in the size and frequency of occurrence of the so-called white layer, resulting in a higher fatigue strength.

Liang et al. [22], distinguished two factors that contribute to the formation of machining stresses. One is the mechanical load during cutting, which generates compressive stresses in the surface layer, and the thermal load, which generates tensile stresses. Progressive tool wear contributes to higher mechanical loads and higher temperatures, which leads to rapid cutting tool destruction. Furthermore, the variation in the distribution of residual stresses depends to a large extent on the cutting parameters, especially the cutting speed v_c, which affects the temperature in the cutting zone and consequently the speed of tool wear. For different combinations of cutting parameters and tool wear, thermal and mechanical loads have different courses, which results in variability of stress directions and values. Regardless of the cutting parameters, the thickness of the near-surface layer, where the occurrence of residual stresses is observed, increases with increasing tool wear.

Rumian et al. [10] found that the knowledge of cutting forces, stresses and temperature in the cutting zone are important elements in the optimization of the machining process of difficult-to-machine alloys. The main indicators of machining quality are the roughness of the machined surface, the values of the components of the total cutting force and the tool wear. In the machining of Inconel 718, intensive tool wear occurs at the initial stage of cutting, which causes a non-linear increase in the specific cutting force k_c, while in sintered nickel superalloys the increase in wear and k_c with increasing length of cut are close to linear. The surface roughness after cutting of sintered nickel alloys increases during cutting (with tool wear) and this tendency is preserved in the studied speed range of 160–200 m/min.

According to Zębala et al [23], during cutting of sintered nickel alloy with a cBN tool, the process of tool wear proceeds in a classical way, i.e. a run-in phase occurs, then the wear stabilizes and in the final phase of tool life a rapid increase of wear is observed. During the cutting process, as the tool wear increased, they recorded a noticeably higher value of the thrust force F_p, the radial component of the cutting force. The research showed the influence of the tool wear on the values of the cutting force components (F_c, F_p, F_f), the specific cutting force k_c, the surface roughness and the form of the chip. Similarly, as stated earlier by W. Grzesik et al., the recommended level of cBN tool wear ensuring relatively low values of cutting force components and good surface quality in machining of sintered superalloys should not exceed 0.2 mm for the wear index VB.

The machining of commonly used nickel-based superalloys such as Inconel 718, Inconel 625 and similar ones has been extensively studied in numerous scientific papers, while studies in the field of machining of nickel- and cobalt-based superalloys obtained by powder metallurgy are scarce. This group is characterized by properties similar to those of the well-known nickel-based superalloys, i.e. low thermal conductivity, tendency to strengthening and the occurrence of hard carbide precipitates, which cause very high thermodynamic loads in the cutting zone, leading to rapid tool wear [1,24]. Wear of the tool affects the properties and structure of the near surface and the resulting residual stresses [25,26].

The objective of this study was to analyze cutting mechanics in terms of changes in the

components of the total cutting force and tool wear and their effect on the consistency of the near surface layer during the turning of a nick-el-cobalt alloy produced by powder metallurgy (PM) using a cBN cutting insert.

MATERIALS AND METHODS

Workpiece material

Cutting tests were conducted on a forging made of a nickel-cobalt-based alloy obtained by powder metallurgy. According to the patent description, the weight composition of this alloy family is as follows [5,6]: Nickel >50%, Cobalt >20% and other alloying elements such as Aluminium 3.10–3. 75%, Boron 0.02–0.09%, Carbon 0.02–0.09%, Chromium 9.50–11.25%, Molybdenum 2.80–4.20%, Niobium 1.60–2.40%, Tantalum 4.20–6.10%, Titanium 2.60–3.50%, Tungsten 1.80–2.50%, Zirconium 0.04–0.09%.

Semifinished products of this family of alloys are obtained by powder metallurgy and then subjected to forging and heat treatment. The use of powder metallurgy makes it possible to achieve greater uniformity of grain size and the subsequent heat treatment after forging significantly influences the favorable form of precipitation strengthening (γ' phase and η phase). An appropriate grain size (preferably 30–60 μm) contributes to an increase in the creep resistance of the material at elevated temperatures and a decrease in susceptibility to crack propagation during operation.

The material is characterized by more favorable strength parameters compared to materials used in previous aircraft engine designs for rotating components in the engine hot zone. The advantage of this group of alloys is particularly evident at temperatures around 649°C, as shown in Table 1 in relation to the popular alloy IN100 [5].

Unfortunately, an unfavorable consequence for subsequent production processes of the final product is the low machinability of this material, which makes the selection of appropriate tools and machining parameters to achieve the desired machining effects a major challenge and significantly affects the cost and time of implementation and production [10,13].

The kinematics of the machining process included radial turning of a face with an outer diameter Ø ≈ 400 mm and an inner diameter Ø ≈ 200 mm. There was a 20 mm × 30° chamfer at the inner diameter, which resulted from the approximation of the demonstrator geometry to the actual aerospace part (Fig. 1).

Cutting tools

The tests were carried out using a VBGW160408 NU2 insert with a cutting edge of cubic boron-nitride (cBN). The cutting edge of the insert was profiled with a 0.06 mm × 20° chamfer for protection against chipping (Fig. 2). The designation CH0620 is used in the following description.

The insert tip was made of cubic boron nitride (cBN) with a fine grain structure, which constitutes 75–80% of the volume of the tool tip material. The cBN grains were bonded with a cobalt-tungsten carbide (WC-Co)-based binder. CBN is the second hardest tool material after diamond and is classified as an advanced tool material which can be successfully used for machining hard-to-machine materials. It exhibits high chemical stability, strength, and wear resistance up to approximately 1000 °C [9,27].

The CE microgeometry measurements for the 4 blades showed the high precision and repeatability of the tool. The range of variation in the results is shown in Table 2.

The cutting inserts were clamped in an SVJBL 2525 M16 toolholder with an internal system to precise coolant feed through the tool to the cutting zone.

Test stand

A CNC lathe NEF 600 was used for the cutting tests, max. OD turning 600 mm, X-travel 1250 mm, main power unit P = 18 kW, n = 3000 RPM, M = 615 Nm, GE Fanuc 210i control system, 8 position VDI 40 tool holder (Fig. 3).

Measurement of cutting force components: main cutting force (F_c), Trust Force (F_p), and feed force (F_f), (Fig. 5), were realized by a Kistler 9257B three-way piezoelectric force gauge with a measuring range ±5 kN, (Fig. 4). Dynamometer attached to the VDI tool holder turret. The signal from the piezoelectric sensors of dynamometer is sent to a Charge Amplifier Kistler 5070A and transmit to an 16-bit analog input module NI 9215 of National Instrument which converts signals to digital from. Digital signals are transferred via USB connector to a PC (Fig. 4) equipped with

Table 1. Properties of the workpiece material (based on [5])

It.	Property	Examined material	IN100
1	Time to rupture, temp. 649°C, load stress 910 MPa;	9380 h	220 h
2	Time to 0,2% creep deformation, temp. 649°C, load stress 910 MPa	470 h	18 h
3	Ultimate tensile strength, temp. 649°C	1510 MPa	1317 MPa
4	Yield strength, temp. 649°C	1062 MPa	931 MPa
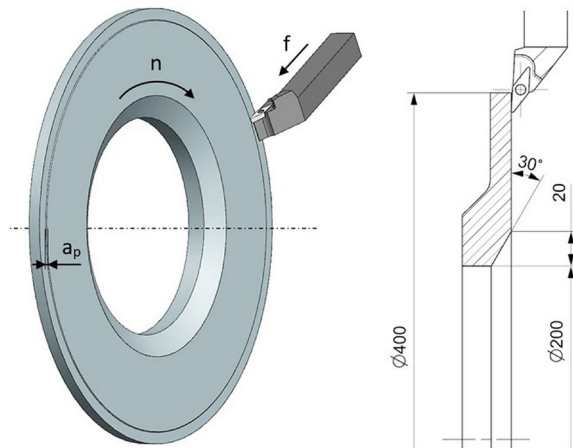
Figure 1. Kinematics of machining trials

custom software for data collection and cutting forces graphical visualization, built on the basis of LabView software. The sampling rate of the signal was set to 10 kHz.

The Ecocool Global 10, semi-synthetic coolant dedicated for the machining of superalloys, was used in this study. Coolant concentration 7–9%, pressure 20 bar. Coolant delivered to the cutting zone through the tool was used (Fig. 6).

An Alicona Infinite Focus G4 microscope was used to determine surface roughness parameters along with software to analyze the scanned surfaces.

Residual stress studies on the machined surface were performed on a Proto iXRD Combo X-ray diffractometer using the XRDWin 2.0.87.17353 software.

Cutting conditions

The selection of parameters for this study was based on the range of parameters used in heat resistant super alloy (HRSA) machining in the industry and the recommendations of the tool manufacturer (Table 3).

RESULTS

The realization of the assumed objective of the research required its division into several stages. In the first stage, the dynamics of cutting tool wear was determined. During the research, tool wear was measured and changes in cutting force components were identified. Then the surface roughness parameters were measured, the influence of the cutting parameters and the tool wear on the stress in the near surface layer was measured.
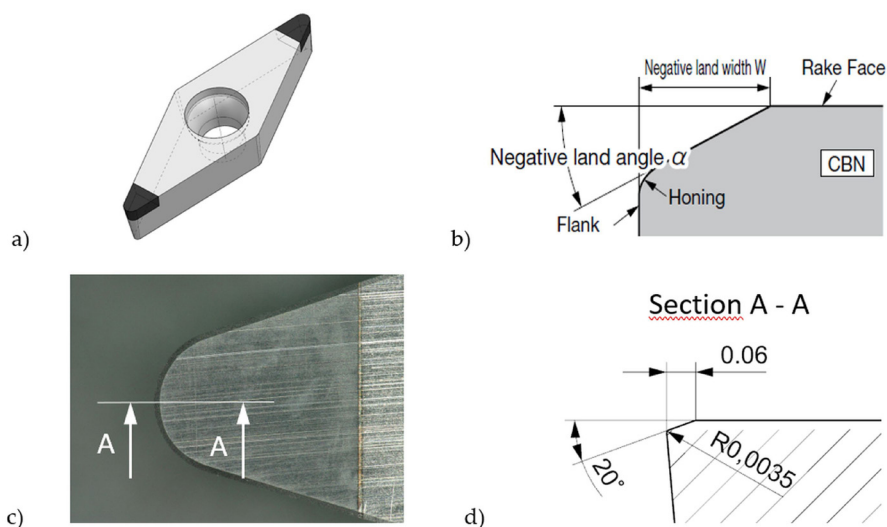
Figure 2. VBGW160408 cutting insert: a) general view, b) chamfer-protected cutting edge profile, c) view of the rake face, d) cutting edge geometry of the tested blade

Table 2. Measurement of the microgeometry of the cutting edge

| It.	Parameter	Nominal value	Measured value	
			Max.	Min.
1	Chamfer length [µm]	60	66.60	66.59
2	Chamfer angle [°]	20	19.60	19.59
3	CE radious [µm]	n/a	3.5	3.5

Tool wear

Due to the possibility of practical application of the research results and recommendations for cBN tools, the wear on the contact surface of about 0.2 mm was adopted as a criterion, which from the point of view of machining critical parts is a value close to, and usually higher than, the value observed in practice for finishing machining of this type of parts. Measurements were made after each working pass. Analyzing the forms of wear occurring during preliminary studies, the indices VB_{Bmax} (maximum width of abrasion traces on the contact surface in the central cutting zone) and VB_N (notch wear at the depth of cut) were selected as the most characteristic forms of wear for the machining case under study (Figure 7).

The first recorded wear measurement was made after the first passage of the tool across the entire width of the machined disc face, i.e., after about 2 minutes of machining. Relatively long passes did not allow to observe the period of "running in" of the tool on the graphs of wear in time.

In the course of the tests and the subsequent wear observations, traces of the characteristic of abrasive wear of the tool were observed in the initial phase of the tests. Notch wear was not yet clearly recognizable at this stage. However, after approx. 5 to 7 minutes, visible notch wear appeared at the depth of cut and became dominant in the subsequent passes (Figure 8). This phenomenon was observed in all the tests conducted. This effect can be attributed to the constant depth of cut and constant feed direction that was used

Figure 3. Test stand – NEF 600 lathe
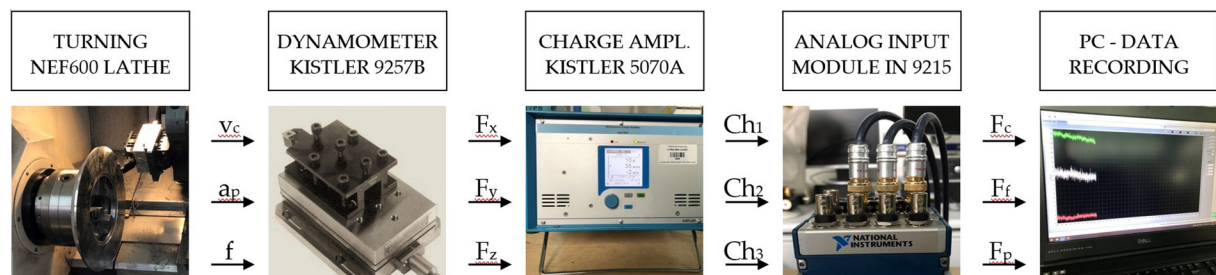
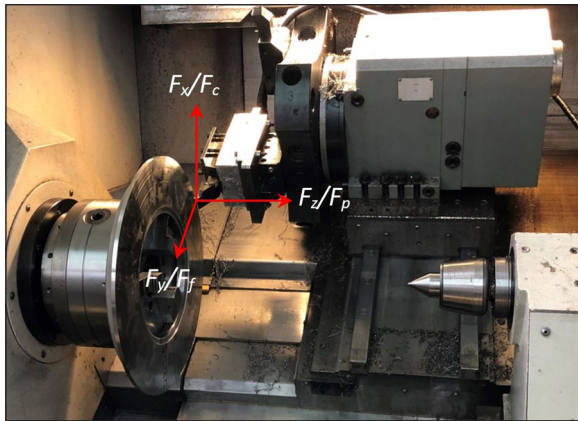**Figure 4.** Configuration of equipment for cutting force components measurements and recording

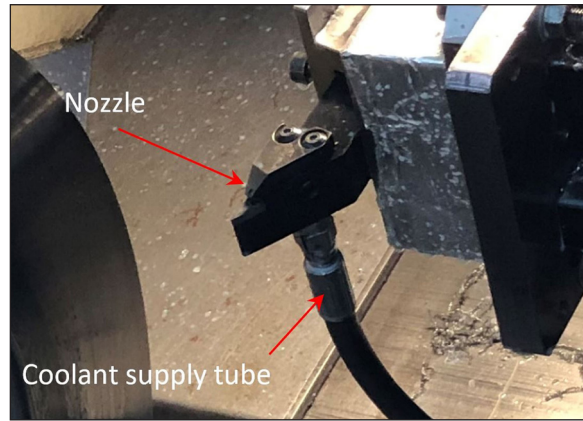**Figure 5.** Force components directions interpretation

Figure 6. Coolant supply to the cutting zone

in the study, as well as the effect of surface layer strengthening due to tool interaction with the workpiece surface, which is characteristic when machining nickel-based superalloys. Certainly, it would be reasonable to use in practice variable depth of cut or turning in different directions so that the layer of material strengthened during cutting 'moves' along the cutting edge on the longest possible section. This would allow to avoid local accumulation of notch wear or even its elimination.

In the final phase of cutting in the P1 test, apart from chipping marks, most probably caused by detachment of an build up edge that tore out a piece of cutting insert material on the contact surface due to strong adhesion, predominant notch wear was observed in the central zone of the abrasion. A similar relationship of notch wear to other forms was observed in the P2 test, except that here there is no evidence of chipping (Figure 9).

Changes in the cutting force components over the life of the tool

Cutting force components were also measured during tool life tests. In all tests, the highest value was recorded for the thrust force F_p and the lowest values for the feed force F_f components of the cutting force. A relatively fast increasing tendency of the examined components of the cutting force was registered in the initial stage of the blade wear, i.e. until reaching VB_{Bmax} in the range

of 0.09 to 0.11 mm or, with respect to VB_N, to the level of about 0.09 mm. Thereafter, a clear stabilization and even a slight decrease in the values of some cutting force components can be seen despite the increase in both forms of tool wear, as can be seen in Figure 10.

When considering the dynamics of the machining force components increase in time, a similar tendency can be seen in Figure 11. After a time of about 5 minutes, all the machining force components stabilize, the graphs "flatten out" and the changes of force F_c and F_f values in time are relatively small. An analogous tendency of decreasing the value of the thrust force can also be observed, as in the previous graphs. It is clearly seen that there is a high convergence of force component values at individual measurement points during both tests, which could not be observed in the previous graphs. When analyzing the force components, it can be concluded that despite the different values of the wear forms in the measurement points for both tests, no dominant influence of the analyzed tool wear parameters

Table 3. Cutting parameters

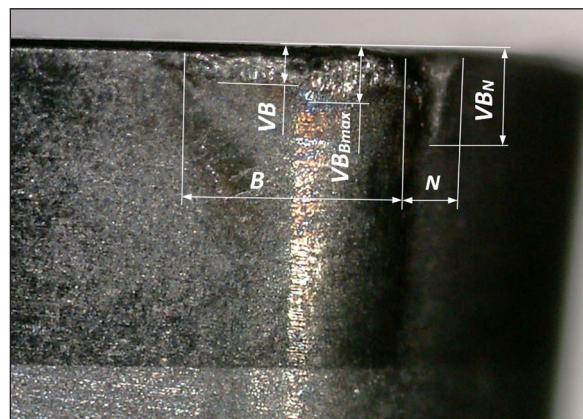| Parameter	Unit	Test parameters value
Cutting speed v_c	m/min	240
Feed rate f	mm/rev	0.10
Depth of cutt a_p	mm	0.11

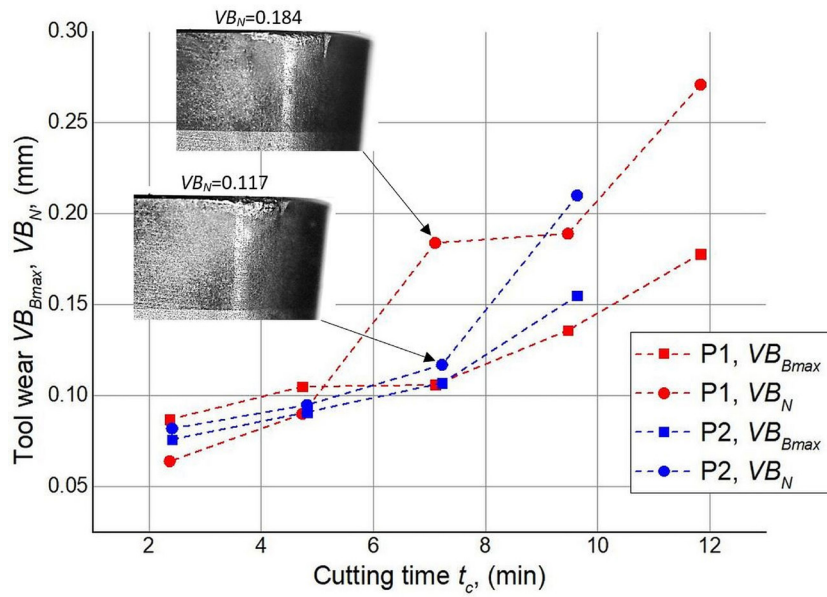**Figure 7.** Registered forms of tool wear

Figure 8. Changes over wear indicators in time with the appearance of the dominant form of notch wear
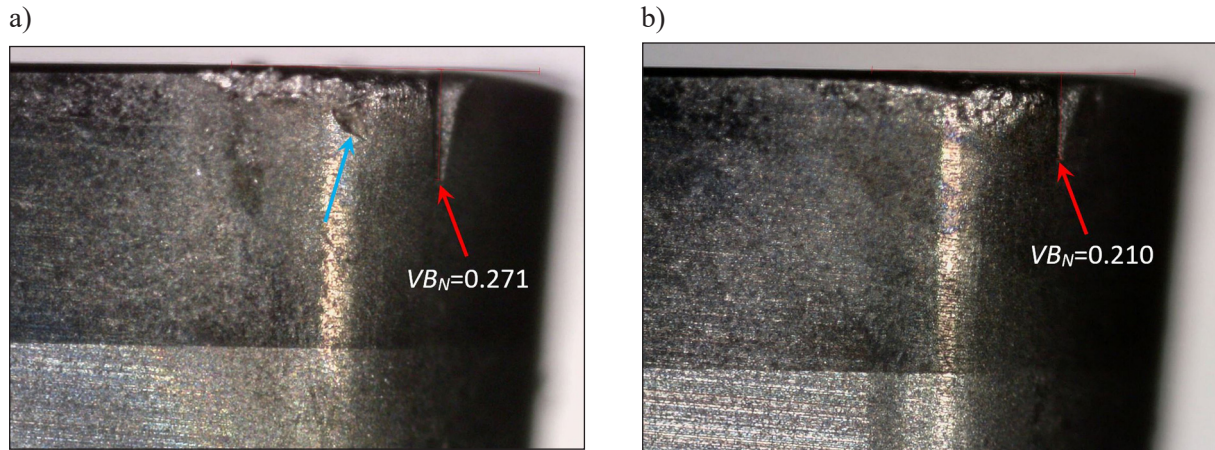

Figure 9. Cutting tool wear CH0620 at the end of test a) P1, b) P2 – clear prevailing notch wear – red arrow and traces of chipping on the P1 insert – blue arrow
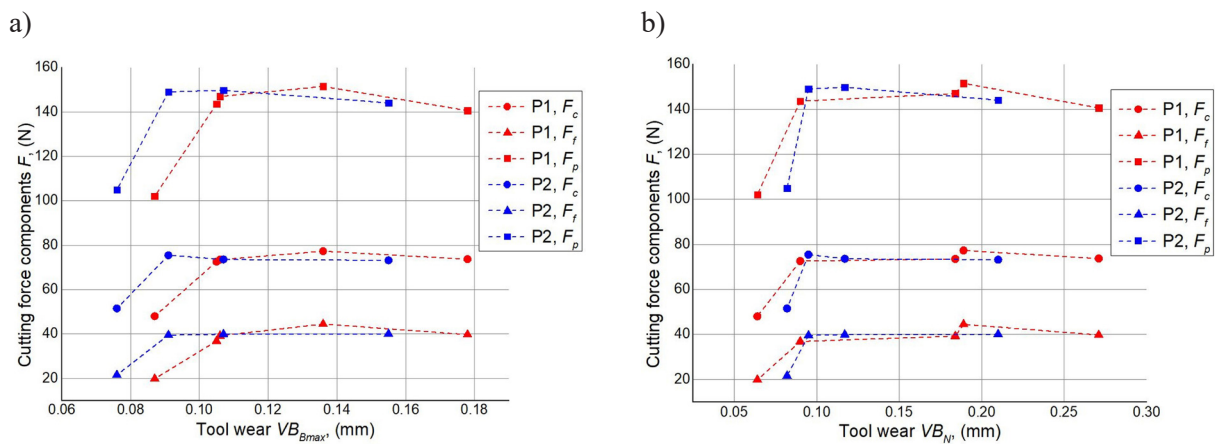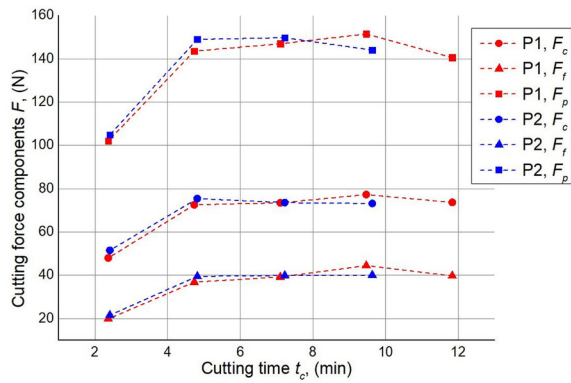

Figure 10. Variation of the cutting force components F_c, F_f and F_p for individual tests with increasing tool wear a) VB_{Bmax}, b) VB_N

Figure 11. Variation of the cutting force components F$_c$, F$_f$ and F$_p$ at time t$_c$

(VB_{Bmax}, VB_N) was found on the values of the total cutting force components.

Surface tests after machining

A great deal of important information regarding the machinability of materials and the phenomena that occur during cutting are provided by surface topography studies [28]. The selected 3D surface roughness parameters *Sa, Sz, Ssk*, and *Sku* were measured. The roughness parameters *Sa* and *Sz* define the amplitude characteristics of the surface, while *Ssk* and *Sku* describe the height value nature of the distribution [29]. In the Table 4 summarizes the values obtained for the roughness parameters for selected cutting and tool wear parameters.

A single surface roughness parameter contains a limited amount of information. Depending on the case, it may be sufficient from a practical point of view, but often only an association of several quantities describing the amplitude values and their nature allows for a more accurate description of the surface and the determination of its predisposition from the point of view of tribological or strength properties or control of the machining process [29,30].

Figure 12 shows the results obtained in the form of graphs. Assuming the smallest effect of

depth of cut on the surface topography, we focused on determining the dependence of roughness parameters *Sa, Sz, Ssk*, and *Sku* on the feed speed *f*, cutting speed v_c, and tool wear *VB*. In order to reduce the influence of the insert wear, cutting tests were carried out on narrow rings (approximately 4 mm wide).
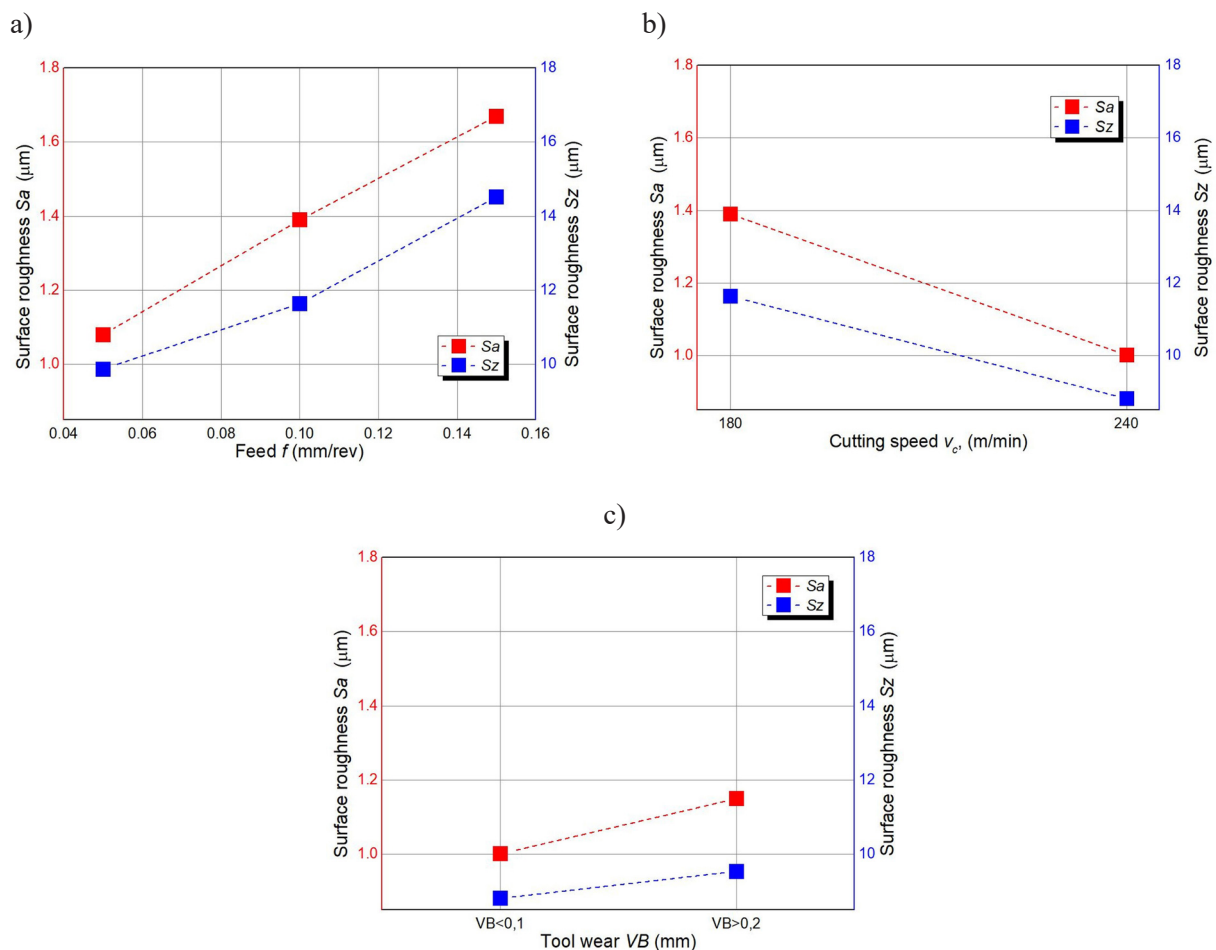
As can be seen, the values of the parameters *Sa* and *Sz* are significantly different (Fig.12 a-c) Both roughness parameters increase with an increase in feed, which results from the kinematic-geometric projection of the tool tip (Fig. 12a). The effect of cutting speed on the values of parameters is also noticeable, with an increase in speed causing a decrease in the roughness *Sa* and *Sz*. This could be due to a greater contribution of plastic phenomena in the process of constituting the surface topography due to an increase in temperature in the cutting zone. The higher temperature formed for higher cutting speeds decreases the value of the plasticizing stress.

A relatively small change in surface roughness was observed between cutting with a new tool (*VB*<0.1) and a worn tool (*VB*>0.2). Larger values of the roughness parameters *Sa* and *Sz* correspond to a higher value of tool wear, which may be related to the almost constant level of cutting forces in this range of tool wear. This could indicate that stabilization of the cutting force components is also associated with stabilization of the phenomena that affect the roughness parameters *Sa* and *Sz*.

The amplitude roughness parameters *Ssk* (skewness) and *Sku* (kurtosis) of the machined surfaces were also analyzed (Fig. 13). Parameters *Ssk* and *Sku* are related to the tribological properties of the surface [28]. The negative value of *Ssk* indicates better surface contact and less friction and wear [29]. Negative *Ssk* was observed for the worn tool VB>0.2 and for the unworn tool and the highest feed value, indicating a significant influence of these variables on the shaping of the surface topography. Taking into account the CE

Table 4. Values of selected 3D surface parameters

Test number	Cutting parameters			Tool wear	Surface parameters			
	v_c, m/min	*f*, mm/rev	a_p, mm	*VB*, mm	*Sa*, µm	*Sz*, µm	*Ssk*, µm	*Sku*, µm
1	180	0.05	0.11	<0.10	1.080	9.870	0.249	3.309
2	180	0.1	0.11	<0.10	1.390	11.640	0.176	2.540
3	180	0.15	0.11	<0.10	1.670	14.520	-0.120	2.790
4	240	0.1	0.11	<0.10	1.001	8.810	0.0056	2.730
5	240	0.1	0.11	>0.20	1.150	9.540	-0.667	3.160

Figure 12. Values of 3D surface roughness parameters Sa and Sz depending on:
a), feed rate, b) cutting speed, c) tool wear

profile (0.06 mm × 20° chamfer), it can be assumed that the relation between the width of the CE protecting chamfer and the feed is crucial here. Both high tool wear and a higher feed rate cause an increase in the proportion of rake area outside the chamfer, which changes the cutting geometry and the process of material decohesion and the elastoplastic interaction of the blade with the machined surface. Positive values of *Ssk* skewness indicate a tendency to initiate friction cracks [29].

A high value of the *Sku* parameter indicates the appearance of many surface defects [28]. From the point of view of the dependence of tribological properties described in the literature, crack initiation on the interacting surfaces, and the number of surface defects, the least favorable is the cutting with a sharp tool at the lowest feed, Fig. 13. This is demonstrated by the positive value of the *Ssk* and *Sku* parameters above 3.0. This is probably the effect of the unfavorable relation of the chamfer size on the CE of the insert to the feed (0.06/0.05; 0.06/0.10), which causes a large plastic impact on the unmachined zones.

Influence of machining conditions on the residual stress on the machined surface

The study of the effect of machining conditions on the tensile stresses on the machined surface was carried out on the face of the disk, turned in the form of consecutive concentric rings with a width of about 4mm with different machining parameters. The stresses were measured in two perpendicular directions, parallel to the radius – measurement marked X, and perpendicular to the radius – measurement marked Y (Table 5).

The dependence of stresses on cutting parameters and tool wear presented in the following shows that residual stresses in the radial direction are compressive in nature and are the dominant form of stress, having values between -425 and -1221 MPa. The stresses in the circumferential direction are mostly tensile, except for the cases for the lowest feed rate and the highest tool wear, and their values do not exceed 400 MPa.

Observing the stress dependence on the feed rate (Fig. 14a), it can be noticed that the radial
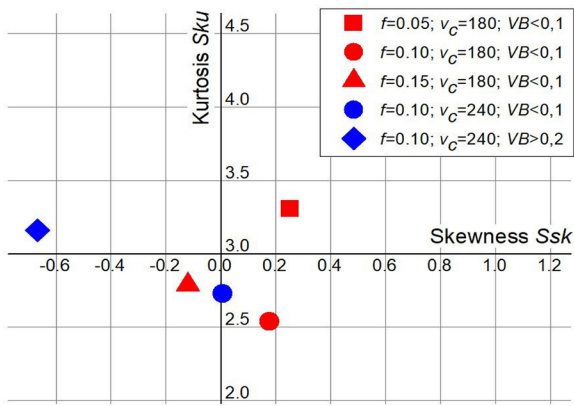
Figure 13. Summary of amplitude 3D surface roughness parameters Sku and Ssk for different values of feed rate, cutting speed, and tool wear

compressive stress decreases proportionally with the increase of the feed rate, while the circumferential stress increases proportionally and quickly changes the direction from compressive (at feed rate f 0.05 mm) to tensile for successive feed rates.

In the graph (Fig. 14b) it can be seen that the cutting speed did not significantly affect the value of radial stresses, they remained almost at the same level, despite a relatively large change in cutting speed (25%). The value of circumferential stresses decreased with an increase in cutting speed, however, their tensile character remained.

Analyzing the influence of cutting edge wear on stress values (Fig. 14c), a small effect can be observed on the radial compressive stresses,

a)

b)

c)
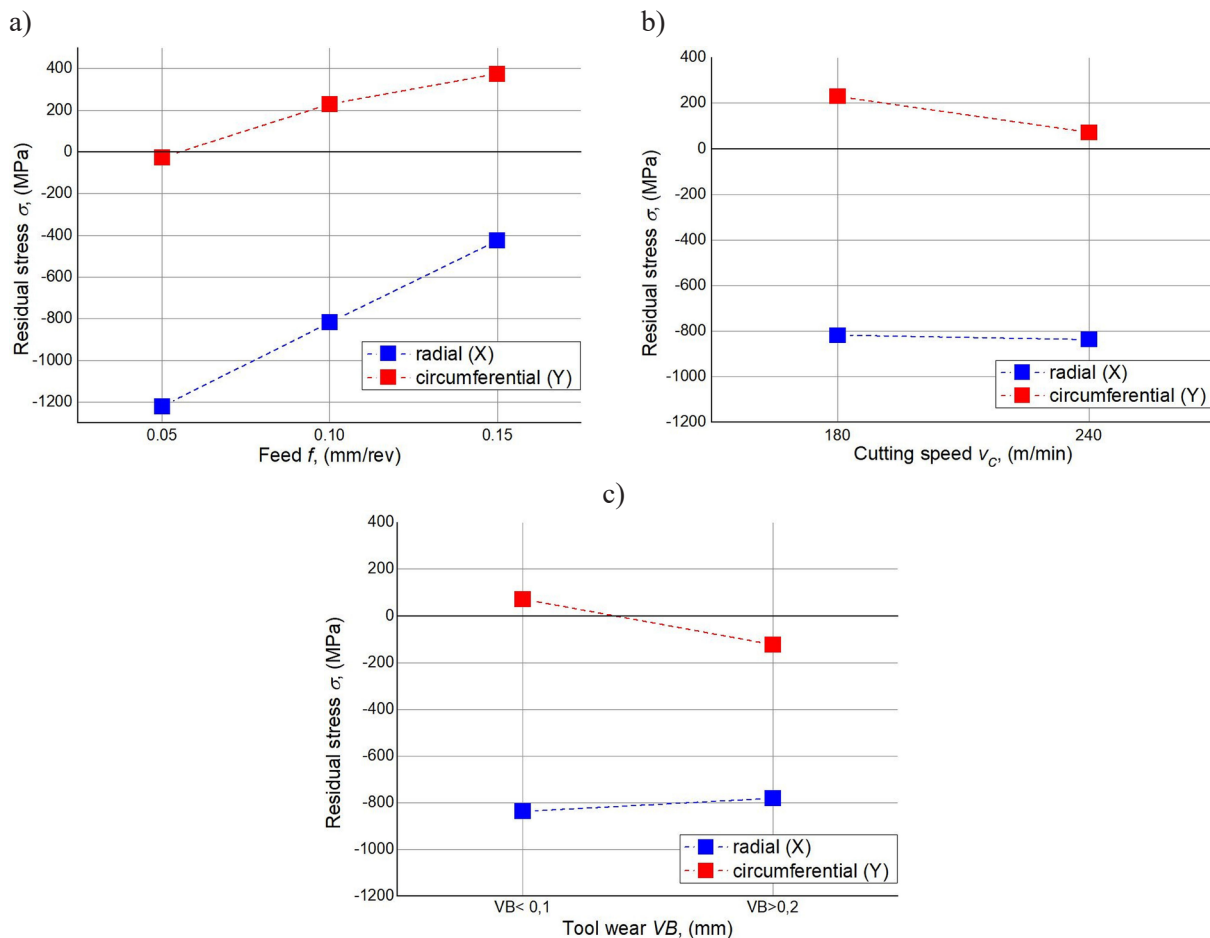
Figure 14. Variation of the value of the surface tensile stresses machined (a) with change in the feed rate, (b) with change in the speed, (c) with change in the blade wear

Table 5. Measured values of surface residual stresses after machining

It.	Cutting parameters			Tool wear	Residual stress X (radial)		Residual stress Y (circumferential)	
	v_c, m/min	f, mm/rev	a_p, mm	VB, mm	σ, MPa	Error, MPa	σ, MPa	Error, MPa
1	180	0.05	0.11	<0.10	-1221	± 20	-26	± 35
2	180	0.1	0.11	<0.10	-818	± 22	230	± 43
3	180	0.15	0.11	<0.10	-425	± 20	376	± 43
4	240	0.1	0.11	<0.10	-837	± 13	72	± 38
5	240	0.1	0.11	>0.20	-781	± 22	-123	± 23

whose value decreased with blade wear. Slightly larger changes can be seen in the circumferential stresses, which change direction from tensile to compressive with tool wear.

Finally, it can be stated that the greatest changes in surface stresses are caused by the change of feed, in this case the values of stresses in both directions change relatively quickly. Tool wear and cutting speed have little effect on radial residual stresses, whereas peripheral stresses change significantly.

CONCLUSIONS

The research conducted made it possible to formulate the following final conclusions.

1. There is a visible tendency for the components of the total cutting force to increase in the initial cutting stage with increasing tool wear, until the values of VB_{Bmax} in the range <0.09; 0.11> mm and VB_N about 0.09 mm are reached. Then, we observe a clear stabilization of the forces, and further wear no longer noticeably affects the change in their values in the range up to VB_{Bmax} about 0.2 mm. The change in tribological conditions is compensated by the change in the actual rake angle as a result of the wear of the chamfer reinforcing the cutting edge.

2. Taking into account the influence of both forms of wear, VB_{Bmax} and VB_N on the components of the total cutting force, it cannot be concluded that either of them has a predominant effect on their values. It can only be observed that the progressive wear of VB_{Bmax} and a significant increase in notch wear in the final phase of the tests do not cause an increase in the cutting forces, and in fact, a slight decrease in the values of some components can be observed.

3. For a sharp tool, the values of the *Sa* and *Sz* parameters increase with an increase in the feed rate, which would mean that at the initial stage of cutting the values of the parameters are mainly related to the kinematic-geometric representation of the tool tip. There is also a positive effect of a higher cutting speed on the values of the roughness parameters *Sa* and *Sz*, which may be related to a greater contribution of plastic phenomena in the process of constituting the surface topography during cutting due to the increase in temperature with an increase in cutting speed. A relatively small change in surface roughness

was observed for a new insert (*VB*<0.1) and a worn one (*VB*>0.2). This may be related to the almost constant level of cutting forces in this range of blade wear, which could indicate that stabilization of the cutting force components is also associated with stabilization of phenomena affecting the *Sa* and *Sz* parameters.

4. From the point of view of the tribological properties of the machined surface, the most favorable values of the parameters *Ssk*<0 and *Sku*<=3 were obtained for medium and high feed values and greater CE wear, which could indicate that a smaller width of the CE reinforcement phase and feeds relatively higher than its value promote the desired surface topography.

5. In the case under consideration, the feed rate has the greatest influence among the examined variables on the tensile stress of the machined surface. Changes in both the radial and circumferential directions show proportional character, with the fact that stresses in the radial direction decrease with an increase of feed rate, whereas in the circumferential direction they increase.

6. The other variables, such as wear and cutting speed, visibly affect only the circumferential stresses, while the radial stresses show small variation.

REFERENCES

1. Choudhury IA., El-Baradie MA. Machinability of nickel-base super alloys: A general review. Journal of Materials Processing Technology 1998; 300(3–4):278–284.

2. Ahmed G.M.S., Mohiuddin M.V., Sultana S., Dora H.K., Singh V.D. Microstructure Analysis and Evaluation of Mechanical Properties of Nickel Based Super Alloy CCA617. Proc. of 4th International Conference on Materials Processing and Characterization, Hyderabad, India 2015; Materials Today 2015; 2(4–5):1260–1269.

3. Thellaputta G.R., Chandra P.S., Rao C.S.P. Machinability of Nickel Based Superalloys: A Review. Proc. of 5th International Conference of Materials Processing and Characterization, Hyderabad, India 2016; Materials Today 2017; 4(2):3712–3721.

4. Polvorosa R., Suárez A., Lacalle LNL de., Cerrillo I., Wretland A., Veiga F. Tool wear on nickel alloys with different coolant pressures : Comparison of Alloy 718 and Waspaloy. Journal of Manufacturing Processes 2017; 26:44–56.

5. Reynolds P.L., Stolz D.S. Superalloy compositions, articles and methods of manufacture. United Technology Corporation, US patent; US 9,783,873 B2, 2017.

6. Reynolds P.L., Stolz D.S. Superalloy compositions, articles and methods of manufacture. United Technology Corporation, EU patent; EP 2 628 810 B1, 2016.

7. Jemielniak K. Review of new developments in machining of aerospace materials. Journal of Machine Engineering 2021; 21(1):22–55.

8. Ramana MV., Mohana Rao GK., Sagar B., Panthangi RK., Ravi Kumar BVR. Optimization of surface roughness and tool wear in sustainable dry turning of Iron based Nickel A286 alloy using Taguchi's method. Cleaner Engineering and Technology 2021; 2:100034.

9. Grzesik W. Podstawy skrawania materiałów konstrukcyjnych. Warszawa: Wydawnictwo Naukowo-Techniczne Sp. z o.o., 2010; 349–370.

10. Rumian K., Zębala W. Optimization of cutting data of nickel-based sintered materials turning. Proc. of Photonics Applications in Astronomy, Communications, Industry, and High-Energy Physics Experiments, Wilga, Poland 2019; 11176:1568–1576.

11. Aerospace Industries Association. Rotor Manufacturing Project Team. Report No. DOT/FAA/AR-06/3: Guidelines to Minimize Manufacturing Induced Anomalies in Critical Rotating Parts 2006.

12. Pratt & Whitney. Materials Control Laboratory Manual E-166 suppl. A 1997, rev. D. 2020.

13. Klocke F., Krämer A., Sangermann H., Lung D. Thermo-mechanical tool load during high performance cutting of hard-to-cut materials. Proc. of 5th CIRP Conference on High Performance Cutting, Zurich, Switzerland 2012, 295–300.

14. Oschelski T.B., Urasato W.T., Amorim H.J., Souza AJ. Effect of cutting conditions on surface roughness in finish turning Hastelloy® X superalloy. Proc. of International Conference on Materials, Processing & Characterization, Mathura, India 2020; Materials Today 2021; 44:532–537

15. Liu R., Eaton E., Yu M., Kuang J. An Investigation of Side Flow during Chip Formation in Orthogonal Cutting. Proc. of 45th SME North American Manufacturing Research Conference, LA, USA 2017; Precedia Manufacturing 2017; 10:568–577.

16. Brown I., Schoop J. An Iterative Size Effect Model of Surface Generation in Finish Machining. Journal of Manufacturing and Materials Processing 2020; 4(3):63.

17. Wojciechowski S. Methods of minimum uncut chip thickness estimation during cutting with defined geometry tools. Mechanik 2018; 91(8–9):664–666.

18. Hood R., Soo S.L., Aspinwall D.K., Mantle A.L. Tool life and workpiece surface integrity when turning an RR1000 nickel-based superalloy. International Journal of Advanced Manufacturing Technology 2018; 98(9–12):2461–2468.

19. Yao C., Zhou Z., Zhang J., Wu D., Tan L. Experimental study on cutting force of face-turning Inconel 718 with ceramic tools and carbide tools. Advances in Mechanical Engineering 2017; 9(7):1–9.

20. Grzesik W., Niesłony P., Habrat W., Sieniawski J., Laskowski P. Investigation of tool wear in the turning of Inconel 718 superalloy in terms of process performance and productivity enhancement. Tribology International 2018; 118:337–346.

21. Sun J., Wang T., Su A., Chen W. Surface integrity and its influence on fatigue life when turning nickel alloy GH4169. Proc. of 4th CIRP Conference on Surface Integrity, Tianjin, China 2018; 71:478–483.

22. Liang X., Liu Z., Wang B. State-of-the-art of surface integrity induced by tool wear effects in machining process of titanium and nickel alloys : A review. Measurement 2019; 132:150–181

23. Zebala W., Struzikiewicz G., Rumian K. Cutting forces and tool wear investigation during turning of sintered nickel-cobalt alloy with CBN tools. Materials 2021; 14(7):1623.

24. Ezugwu EO. Key improvements in the machining of difficult-to-cut aerospace superalloys. International Journal of Machine Tools and Manufacture 2005; 45(12–13):1353–1367.

25. Muñoz-Sánchez A., Canteli JA., Cantero JL., Miguélez MH. Numerical analysis of the tool wear effect in the machining induced residual stresses. Simulation Modelling Practice and Theory 2011; 19(2):872–886.

26. Srinivas K., Devaraj C. Optimization of Residual Stresses in Hard Turning of Super Alloy Inconel 718. Proc. of 7th International Conference of Materials Processing and Characterization, Telangana, India 2017; Materials Today 2018; 5(2):4592–4600.

27. Jemielniak K. Obróbka Skrawaniem-podstawy, dynamika, diagnostyka. Warszawa: Oficyna wydawnicza Politechniki Warszawskiej, 2018.

28. Habrat W. Analiza i modelowanie toczenia wykończeniowego tytanu i jego stopów. Rzeszow: Oficyna wydawnicza Politechniki Rzeszowskiej, 2019.

29. Pawlus P., Reizer R., Wieczorowski M. Functional importance of surface texture parameters. Materials. MDPI 2021; 14(18): 5326

30. Bigerelle M., Najjar D., Mathia T., Iost A., Coorevits T., Anselme K. An expert system to characterise the surfaces morphological properties according to their tribological functionalities: The relevance of a pair of roughness parameters. Tribology International 2013; 59:190–202